

Threshold of primordial black hole formation

¹Tomohiro Harada,* ²Chul-Moon Yoo, and ^{3,4}Kazunori Kohri

¹*Department of Physics, Rikkyo University, Toshima, Tokyo 171-8501, Japan*

²*Gravity and Particle Cosmology Group,*

Division of Particle and Astrophysical Science,

Graduate School of Science, Nagoya University,

Furo-cho, Chikusa-ku, Nagoya 464-8602, Japan

³*Theory Center, Institute of Particle and Nuclear Studies,*

KEK (High Energy Accelerator Research Organization),

1-1 Oho, Tsukuba 305-0801, Japan and

⁴*The Graduate University for Advanced Studies (Sokendai),*

1-1 Oho, Tsukuba 305-0801, Japan

(Dated: November 7, 2018)

Abstract

Based on a physical argument, we derive a new analytic formula for the amplitude of density perturbation at the threshold of primordial black hole formation in the Universe dominated by a perfect fluid with the equation of state $p = w\rho c^2$ for $w \geq 0$. The formula gives $\delta_{Hc}^{\text{UH}} = \sin^2[\pi\sqrt{w}/(1+3w)]$ and $\tilde{\delta}_c = [3(1+w)/(5+3w)]\sin^2[\pi\sqrt{w}/(1+3w)]$, where δ_{Hc}^{UH} and $\tilde{\delta}_c$ are the amplitude of the density perturbation at the horizon crossing time in the uniform Hubble slice and the amplitude measure used in numerical simulations, respectively, while the conventional one gives $\delta_{Hc}^{\text{UH}} = w$ and $\tilde{\delta}_c = 3w(1+w)/(5+3w)$. Our formula shows a much better agreement with the result of recent numerical simulations both qualitatively and quantitatively than the conventional formula. For a radiation fluid, our formula gives $\delta_{Hc}^{\text{UH}} = \sin^2(\sqrt{3}\pi/6) \simeq 0.6203$ and $\tilde{\delta}_c = (2/3)\sin^2(\sqrt{3}\pi/6) \simeq 0.4135$. We also discuss the maximum amplitude and the cosmological implications of the present result.

PACS numbers: 04.70.Bw, 97.60.Lf, 95.35.+d

* harada@rikkyo.ac.jp

I. INTRODUCTION

Primordial black holes may have formed from primordial fluctuations in the early Universe [1, 2]. Since primordial black holes can in principle be observed at the present epoch, current observations constrain the abundance of primordial black holes and thereby primordial fluctuations. In other words, primordial black holes can be used as a probe into the early Universe. This kind of analysis was first implemented by Carr [3]. See Carr *et al.* [4] for its latest update.

To constrain early Universe scenarios from the observational constraint of primordial black holes, the formation threshold of the primordial black hole is very important. The conventional condition known as Carr's [3] is that a primordial black hole is formed if and only if the density perturbation δ_H when the fluctuation enters the horizon is in the range $w = \delta_c < \delta_H < \delta_{\max} = 1$, where the equation of state $p = w\rho c^2$ is assumed. Although uncertainties in numerical factors of order unity in both the threshold and maximum values were noticed in the original paper, the uncertainties have often been omitted in the subsequent literature. However, the uncertainty of factor 2 in the threshold value δ_c results in enormous uncertainty in the prediction of the abundance of primordial black holes if we are given the power spectrum of the density perturbation because δ_c should be much greater than the standard deviation σ . The maximum value δ_{\max} , which was originally regarded as the separate universe condition [5], has recently been shown [6, 7] to be purely geometrical.

Since Nadezhin, Novikov, and Polnarev [8, 9] pioneered the fully general relativistic numerical simulations of primordial black hole formation, the threshold of primordial black hole formation has been extensively investigated by numerical relativity [10–15]. Niemeyer and Jedamzik [10] reported the threshold value $\delta_c \simeq 0.67 - 0.71$, which was later revised to the value $\simeq 0.43 - 0.47$ with a purely growing mode by Musco, Miller, and Rezzolla [12]. The latest value for a radiation fluid is given by $\delta_c \simeq 0.45 - 0.47$ and $\simeq 0.48 - 0.66$ depending on the parametrization of curvature profiles, as shown in Figs. 10 and 11 of Polnarev and Musco [13]. Moreover, Musco, and Miller [15] presented the numerical simulations of primordial black hole formation and the threshold values obtained for different values of w in the range $0.01 \leq w \leq 0.6$.

Khlopov and Polnarev [17] pioneered the production of primordial black holes in the matter-dominated phase, where $w = 0$, in the context of grand unification. In the context of

modern inflationary cosmology, the production of primordial black holes is interesting not only in the radiation-dominated phase but also immediately after the inflationary phase, where $w \ll 1$ is effectively satisfied. Suyama *et al.* [18, 19] showed that primordial black holes cannot be overproduced during the resonant preheating phase after the inflation but the production can be significantly enhanced in the universe undergoing tachyonic preheating. Alabidi *et al.* [20, 21] discussed primordial black hole formation in the matter-dominated phase immediately after the inflation, where the formation efficiency may be enhanced by the softness of the equation of state but suppressed due to the effects of nonspherical collapse dynamics.

In the current paper, we derive a new analytic formula for the threshold of primordial black hole formation for general values of w for $w \geq 0$ based on a physical argument. For this purpose, we use a spherically symmetric model of a uniform overdensity surrounded by an underdense compensating layer in the flat Friedmann background. Fixing a gauge problem, we then see a very good agreement of our analytic formula with the numerical result by Musco and Miller [15] both qualitatively and quantitatively.

This paper is organized as follows. In Sec. II, we briefly summarize the original analysis of the condition for primordial black hole formation. In Sec. III, we present our analytic model, derive a matter-independent maximum amplitude of the density perturbation and discuss apparent horizons in this model. In Sec. IV, we analyze the threshold of primordial black hole formation in the matter-dominated universe and in the universe dominated by a perfect fluid. In the latter case, we derive a new analytic expression for the threshold value. In Sec. V, we clarify the gauge problem and compare our analytic formula with the numerical result. In Sec. VI, we discuss the probability distribution of perturbations. Section VII is devoted to summary. We follow the metric signature $(-, +, +, +)$ and the abstract index notation by Wald [25].

II. BRIEF SUMMARY OF THE ORIGINAL ANALYSIS

The original analysis by Carr [3] is based on the physical argument that for an overdensity to form a primordial black hole, the size of the overdensity at the maximum expansion R_{\max} should be larger than the Jeans radius R_J (the Jeans criterion) but smaller than the particle horizon size R_{PH} , which is comparable with the curvature scale of the overdense region. The

maximum size was considered as necessary for the overdense region not to be separated from the rest of the universe [5]. This implies

$$R_J \lesssim R_{\max} \lesssim R_{\text{PH}}. \quad (2.1)$$

Note that the particle horizon size is given by $R_{\text{PH}} \sim c/\sqrt{8\pi G\rho_{\max}/3}$, while the Jeans radius is given by $R_J \sim \sqrt{w}R_{\text{PH}}$, where ρ_{\max} is the density of the overdense region at the maximum expansion and the equation of state $p = w\rho c^2$ is assumed. The condition (2.1) implies that the density perturbation δ_0 of mass scale M at $t = t_0$ must satisfy

$$w \left(\frac{M}{M_{H_0}} \right)^{-2/3} \lesssim \delta_0 \lesssim \left(\frac{M}{M_{H_0}} \right)^{-2/3}, \quad (2.2)$$

where M_{H_0} is the mass enclosed within the horizon at $t = t_0$. This roughly gives

$$w \simeq \delta_c \lesssim \delta_H \lesssim \delta_{\max} \simeq 1, \quad (2.3)$$

where δ_H is the density perturbation at the horizon crossing and δ_c and δ_{\max} denote the threshold value and the maximum value of δ_H for primordial black hole formation, respectively. This is often known as Carr's condition for primordial black hole formation. For a radiation fluid $w = 1/3$, this gives the often quoted value $\delta_c \simeq 1/3$. A more precise argument to derive this condition will be described later in this paper.

As Carr [3] indicated, if the equation of state is sufficiently soft, nonspherical effects play important roles rather than the Jeans criterion. Kopp, Hofmann, and Weller [6] pointed out that the maximum value δ_{\max} is not directly related to the separate universe but to the geometry of the overdense region.

III. DENSITY PERTURBATION MODEL AND THE MAXIMUM AMPLITUDE

A. Three-zone model

Here we introduce a spherically symmetric model of density perturbation, which we will use for the analytic derivation of the formation threshold and the maximum amplitude. The model is schematically depicted in Fig. 1.

The background universe is given by a flat Friedmann solution

$$ds^2 = -c^2 dt^2 + a_b^2(t)(dr^2 + r^2 d\Omega^2), \quad (3.1)$$

where $d\Omega^2$ is the line element on the unit two-sphere. The Friedmann equation is given by

$$\left(\frac{\dot{a}_b}{a_b}\right)^2 = \frac{8\pi G\rho_b}{3}, \quad (3.2)$$

where ρ_b is the mass density of the background universe. The overdense region is described by a closed Friedmann solution

$$ds^2 = -c^2 dt^2 + a^2(t)(d\chi^2 + \sin^2 \chi d\Omega^2) \quad (3.3)$$

or

$$ds^2 = -c^2 dt^2 + a^2(t) \left(\frac{dr^2}{1 - Kr^2} + r^2 d\Omega^2 \right), \quad (3.4)$$

where $K = 1$ and $r = \sin \chi$. The Friedmann equation is given by

$$\left(\frac{\dot{a}}{a}\right)^2 = \frac{8\pi G\rho}{3} - \frac{c^2}{a^2}, \quad (3.5)$$

where ρ is the mass density of the overdense region. The overdensity is surrounded by an underdense layer which compensates the overdensity. We adopt a model where the overdense region is described by a closed Friedmann solution for $0 < \chi < \chi_a$, the surrounding underdense layer is matched with the overdense region at $\chi = \chi_a$, and the further surrounding flat Friedmann solution is matched with the compensating layer at $r = r_b$. Thus, the areal radius of the overdense region is given by $R_a = a \sin \chi_a$, while that for the matching surface between the compensating layer and the flat Friedmann universe is given by $R_b = a_b r_b$. We call fluctuations with $0 < \chi_a < \pi/2$ and $\pi/2 < \chi_a < \pi$ types I and II, respectively, according to the notation of Kopp, Hofmann, and Weller [6]. We note that the coordinates in Eq. (3.4) cannot entirely cover the overdense region of type II fluctuation.

This model can be exact only for the dust case. In other cases, inhomogeneity will penetrate the homogeneous regions through sound waves. To keep the model exact, we would need to introduce some unphysical matter field or shell in the compensating region. We here use this model, which can be called a “three-zone” model, to obtain the threshold value of primordial black hole formation. This model can be justified at least for $w \ll 1$, where the effect of pressure gradient force is very small. It can also be justified at least in the early stage of evolution because in the absence of decaying mode the inhomogeneity will be locally described by a homogeneous solution at each spatial point and the pressure gradient force can be neglected in accordance with the Belinsky–Khalatnikov–Lifshitz conjecture [22, 23].

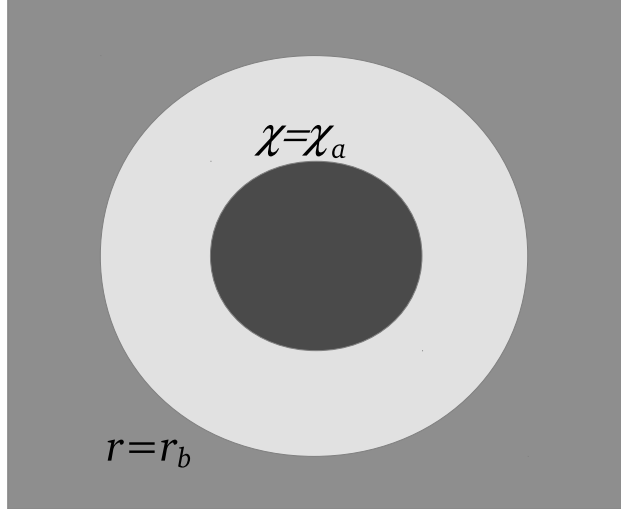


FIG. 1. The schematic figure of the three-zone model of density perturbation.

B. Maximum amplitude of the density perturbation

For convenience, we define the time-dependent density parameter Ω of the overdense region by

$$\Omega = \frac{8\pi G\rho}{3H^2} = 1 + \frac{c^2}{a^2 H^2}, \quad (3.6)$$

where $H = \dot{a}/a$ is the Hubble parameter and we have used Eq. (3.5) in the last equality. Defining the Hubble horizon radius $R_H = cH^{-1}$ in the overdense region, Eq. (3.6) can be transformed to

$$(\Omega - 1) \left(\frac{R_a}{R_H} \right)^2 = \sin^2 \chi_a. \quad (3.7)$$

This implies the left-hand side is time-independent and coincides with $\sin^2 \chi_a$. The density perturbation δ of the overdense region to the background universe is defined by

$$\delta = \frac{\rho - \rho_b}{\rho_b}. \quad (3.8)$$

The density parameter Ω can then be related to δ according to

$$\Omega = (1 + \delta) \left(\frac{H_b}{H} \right)^2, \quad (3.9)$$

where $H_b = \dot{a}_b/a_b$ is the background Hubble parameter and Eqs. (3.2) and (3.6) are used. It should be noted that the above relation is exact. Ω is gauge-independent, while both δ and H_b are gauge-dependent.

The horizon crossing time is defined by the equality between the areal radius of the overdense region, R_a , and the Hubble horizon of the background flat Friedmann universe, $R_{H_b} = cH_b^{-1}$. Equations (3.7) and (3.9) imply that the density perturbation δ_H at the horizon crossing time is given by

$$\delta_H = \left(\frac{H}{H_b}\right)^2 - \cos^2 \chi_a, \quad (3.10)$$

which trivially satisfies

$$\left(\frac{H}{H_b}\right)^2 - 1 < \delta_H \leq \left(\frac{H}{H_b}\right)^2. \quad (3.11)$$

The maximum value is taken only for $\chi_a = \pi/2$, where the overdense region is a three-hemisphere. The lower limit corresponds to both $\chi_a = 0$ and π , and the latter corresponds to the separate universe limit of the overdense region. The inequality (3.11) is automatically satisfied only if we assume the overdense region. One value for δ_H generally corresponds to two distinct configurations, the one of type I and the other of type II. The maximum density does not correspond to the separate-universe configuration $\chi_a = \pi$, as indicated by Kopp, Hofmann, and Weller [6].

We can take a time slice on which the Hubble constants are the same between the overdense and the background regions, i.e., $H = H_b$. We call this time slice the uniform Hubble slice. This is the case in the constant mean curvature slice, which is taken by Shibata and Sasaki [11].

In the uniform Hubble slice, Eq. (3.9) implies that the time-dependent density parameter Ω and the density perturbation δ are directly related, i.e.,

$$\Omega = 1 + \delta^{\text{UH}}, \quad (3.12)$$

where δ^{UH} denotes δ in the uniform Hubble slice. Equation (3.7) then implies

$$\delta^{\text{UH}} \left(\frac{R_a}{R_H}\right)^2 = \delta_H^{\text{UH}} = \sin^2 \chi_a. \quad (3.13)$$

Therefore, $\delta^{\text{UH}}(R_a/R_{H_b})^2$ is time-independent and coincides with δ_H^{UH} . It immediately follows

$$0 < \delta_H^{\text{UH}} \leq 1, \quad (3.14)$$

where $\delta_H^{\text{UH}} = 1$ holds only for $\chi_a = \pi/2$. The above conclusion does not depend on the equations of state or even the matter fields. The analysis does not invoke any linearization

with respect to the amplitude of the density perturbation. It should be noted that we do not need to assume even the existence of maximum expansion here, although we will discuss it later in a different context.

If there is a maximum expansion phase of the overdense region, Eq. (3.5) implies

$$a_{\max} = \frac{c}{\sqrt{8\pi G\rho_{\max}/3}}, \quad (3.15)$$

where ρ_{\max} is the density of the overdense region at the maximum expansion. In other words, a_{\max} coincides with the Hubble horizon radius of the background flat Friedmann universe in the uniform density slice.

C. Trapped surfaces and apparent horizons

In spherically symmetric spacetimes, we have a well-behaved quasilocal mass, which is called the Misner–Sharp mass [26]. The Misner–Sharp mass M is defined as

$$M = \frac{c^2}{2G}R(1 - g^{ab}\nabla_a R\nabla_b R), \quad (3.16)$$

where R is the areal radius. This is closely related to the outgoing and ingoing null expansions, θ_+ and θ_- , respectively, where and hereafter we assume $\theta_+ \geq \theta_-$ without loss of generality [27]. If $2GM/(c^2R) > 1$, we have $\theta_+\theta_- > 0$. A surface on which $\theta_+\theta_- > 0$ is called a trapped surface. A surface on which both θ_+ and θ_- are negative (positive) is said to be future (past) trapped. If $2GM/(c^2R) < 1$, we have $\theta_+\theta_- < 0$. A surface on which $\theta_+\theta_- < 0$ is said to be untrapped. If $2GM/(c^2R) = 1$, we have $\theta_+\theta_- = 0$. A surface on which $\theta_+\theta_- = 0$ is called a marginal surface or an apparent horizon¹. A surface on which $\theta_+ = 0$ and $\theta_- < 0$ ($\theta_+ > 0$ and $\theta_- = 0$) is called a future (past) apparent horizon. A future apparent horizon implies that no null geodesic congruence has positive expansion on it, which suggests the formation of a black hole. If the spacetime is asymptotically flat, the existence of a future apparent horizon implies the existence of a future event horizon outside or coinciding with it [28]. In fact, even if the spacetime is not asymptotically flat, a future apparent horizon can be regarded as a black hole horizon. See Ref. [27] for more rigorous terminology, definitions and proofs.

¹ Strictly speaking, the notion of an apparent horizon depends on the choice of a Cauchy surface on which it is defined. We here take the $t = \text{const.}$ surface as a Cauchy surface.

In the closed Friedmann spacetime, the areal radius and the Misner–Sharp mass are given by $R = a \sin \chi$ and

$$M = \frac{c^2}{2G} a \left[1 + \left(\frac{\dot{a}}{c} \right)^2 \right] \sin^3 \chi, \quad (3.17)$$

respectively. Since

$$\frac{2GM}{c^2 R} = \left[1 + \left(\frac{\dot{a}}{c} \right)^2 \right] \sin^2 \chi, \quad (3.18)$$

the apparent horizon, where $2GM/(c^2 R) = 1$, is given by a two-sphere

$$\sin \chi = \left[1 + \left(\frac{\dot{a}}{c} \right)^2 \right]^{-1/2}. \quad (3.19)$$

At the maximum expansion, there is a marginally trapped surface at $\chi = \pi/2$ or a great sphere. From Eqs. (3.18) and (3.19), it follows that any type II fluctuation immediately after the maximum expansion necessarily has future trapped surfaces, where $2GM/(c^2 R) > 1$, including $\chi = \pi/2$, and a future apparent horizon at $\chi \in (\pi/2, \chi_a)$ which is given by Eq. (3.19).

IV. THRESHOLD OF PRIMORDIAL BLACK HOLE FORMATION

A. Matter-dominated universe

In this section, we assume that the matter field is a dust, where our three-zone model is exact. The Friedmann equation for the overdense region is then given by

$$\dot{a}^2 = \frac{A}{a} - c^2, \quad (4.1)$$

where $A = 8\pi G \rho_0 a_0^3/3$ with $\rho = \rho_0$ and $a = a_0$ at $t = t_0$. The solution of Eq. (4.1) is given by

$$a = \frac{a_{\max}}{2}(1 - \cos \eta), \quad t = \frac{t_{\max}}{\pi}(\eta - \sin \eta), \quad (4.2)$$

where a_{\max} and t_{\max} are given in terms of a_0 and Ω_0 as follows:

$$a_{\max} = \frac{\Omega_0}{\Omega_0 - 1} a_0 = \frac{\Omega_0}{(\Omega_0 - 1)^{3/2}} c H_0^{-1}, \quad t_{\max} = \frac{\pi}{2} \frac{a_{\max}}{c}, \quad (4.3)$$

where Eq. (3.6) is used.

The apparent horizon in the overdense region is given by

$$\eta = 2\chi \quad \text{and} \quad \eta = 2\pi - 2\chi. \quad (4.4)$$

If we concentrate on type I fluctuation, i.e., $0 < \chi_a < \pi/2$, the future apparent horizon corresponds to $\eta = 2\pi - 2\chi$. Let us assume that a future apparent horizon exists when the overdense region shrinks to f ($0 < f < 1$) times the maximum expansion, i.e., $a/a_{\max} = f$. Then, Eqs. (3.19) and (4.1) yield

$$\chi_a > \arcsin\sqrt{f}. \quad (4.5)$$

At the maximum expansion, the areal radius of the overdense region is given by

$$R_{a,\max} = a_{\max} \sin \chi_a. \quad (4.6)$$

This cannot be greater than a_{\max} . The combination of Eqs. (4.5) and (4.6) means

$$\sqrt{f}a_{\max} < R_{a,\max} \leq a_{\max}. \quad (4.7)$$

Since we can rewrite $R_{a,\max}$ as

$$R_{a,\max} = a_{\max} \sin \chi_a = \frac{\Omega_0}{\Omega_0 - 1} a_0 \sin \chi_a = \frac{\Omega_0}{\Omega_0 - 1} R_{a,0}, \quad (4.8)$$

where $R_{a,0} = a_0 \sin \chi_a$ is the areal radius of the overdense region at $t = t_0$, using Eq. (4.3) we find

$$f < (\Omega_0 - 1) \left(\frac{R_{a,0}}{R_{H_0}} \right)^2 \leq 1, \quad (4.9)$$

where $R_{H_0} = cH_0^{-1}$. This is the condition for primordial black hole formation in terms of the quantities at $t = t_0$. The above condition is exact, although the factor f is left unspecified.

It is a convention to express the condition for primordial black hole formation in terms of the density perturbation δ_H at the horizon crossing. As we have seen, $(\Omega_0 - 1) (R_{a,0}/R_{H_0})^2$ is equal to the density perturbation δ_H^{UH} at the moment of horizon crossing in the uniform Hubble slice. Equation (4.9) can then be reduced to the condition in terms of δ_H^{UH} as follows

$$f < \delta_H^{\text{UH}} \leq 1. \quad (4.10)$$

In the dust case, f should be determined by considering the effects, such as caustics, inhomogeneity, and deviations from spherical symmetry inside the overdense region; these effects can strongly affect the collapse dynamics and then prevent the overdense region from becoming a black hole at the moment before the overdense region shrinks to f times the maximum expansion. These effects have been discussed by Khlopov and Polnarev [17].

B. Universe dominated by a perfect fluid with $p = w\rho c^2$

1. Jeans radius and Carr's threshold

We will see how the primordial black hole formation condition against the pressure gradient force is obtained with the three-zone model. We assume the equation of state $p = wc^2\rho$ ($w > 0$). Except for $w \ll 1$, we can expect that the Jeans criterion gives the threshold of black hole formation rather than the nonspherical effects. For this case, the flat Friedmann solution is given by

$$a_b \propto t^{2/(3(1+w))}. \quad (4.11)$$

The Friedmann equation for the overdense region is given by

$$\dot{a}^2 = Aa^{-(1+3w)} - c^2, \quad (4.12)$$

where A is given by

$$A = \frac{8\pi}{3}G\rho_0 a_0^{3(1+w)}, \quad (4.13)$$

with $\rho = \rho_a$ and $a = a_0$ at $t = t_0$.

At the maximum expansion, the areal radius of the overdense region is given by

$$R_{a,\max} = a_{\max} \sin \chi_a. \quad (4.14)$$

This cannot be greater than a_{\max} due to spherical geometry, while this must be greater than the Jeans radius R_J of the overdense region at maximum expansion.

$$R_J < R_{a,\max} \leq a_{\max}. \quad (4.15)$$

The precise estimate of R_J is not a trivial task. The standard Newtonian argument of the Jeans instability in a static and uniform gas cloud gives

$$R_J = c_s \sqrt{\frac{\pi}{G\rho}}, \quad (4.16)$$

where ρ and c_s are the density and the sound speed of the background uniform gas cloud, respectively. We may replace c_s with $\sqrt{w}c$ in the present case. Now we can adopt the following choice:

$$R_J = \sqrt{w}c \frac{1}{\sqrt{8\pi G\rho_{\max}/3}} = \sqrt{w}a_{\max}. \quad (4.17)$$

Note that this is \sqrt{w} times the Hubble radius of the background flat Friedmann universe in the uniform density slice.

Since Eqs. (3.6), (4.12) and (4.13) yield

$$\frac{a_{\max}}{a_0} = \left(\frac{\Omega_0}{\Omega_0 - 1} \right)^{1/(1+3w)} \quad (4.18)$$

and

$$a_0 = (\Omega_0 - 1)^{-1/2} cH_0^{-1}, \quad (4.19)$$

Eq. (4.15) gives the following exact relation:

$$w < (\Omega_0 - 1) \left(\frac{R_{a,0}}{R_{H_0}} \right)^2 \leq 1. \quad (4.20)$$

Since

$$(\Omega_0 - 1) \left(\frac{R_{a,0}}{R_{H_0}} \right)^2 = \delta_H^{\text{UH}} \quad (4.21)$$

again, we find the following condition for primordial black hole formation:

$$w < \delta_H^{\text{UH}} \leq 1. \quad (4.22)$$

However, this is clearly dependent on the choice of R_J . In other words, it is the choice of R_J given by Eq. (4.17) that reproduces Carr's threshold.

2. Refining the threshold

It should be noted again that there is some ambiguity in the choice of the Jeans radius in Eq. (4.17) by a numerical factor of order unity. Here we develop a physical argument to determine the numerical factor of the threshold value.

Defining the new variables \tilde{a} and \tilde{t} [7, 24] such that

$$\tilde{a} = a^{1+3w}, \quad d\tilde{t} = (1 + 3w)\tilde{a}^{3w/(1+3w)} dt, \quad (4.23)$$

we can transform Eq. (4.12) into the dust form:

$$\left(\frac{d\tilde{a}}{d\tilde{t}} \right)^2 = \frac{A}{\tilde{a}} - c^2. \quad (4.24)$$

This can be integrated to give the parametric form of the solution,

$$\tilde{a} = \tilde{a}_{\max} \frac{1 - \cos \eta}{2}, \quad \tilde{t} = \tilde{t}_{\max} \frac{\eta - \sin \eta}{\pi}, \quad (4.25)$$

where \tilde{a}_{\max} and \tilde{t}_{\max} are given as follows:

$$\tilde{a}_{\max} = \frac{\Omega_0}{\Omega_0 - 1} \tilde{a}_0, \quad \tilde{t}_{\max} = \frac{\pi \tilde{a}_{\max}}{2c}. \quad (4.26)$$

Using the (η, χ) coordinates, the line element can be rewritten in the form

$$ds^2 = \tilde{a}^{2/(1+3w)} \left[-\frac{1}{(1+3w)^2} d\eta^2 + d\chi^2 + \sin^2 \chi d\Omega^2 \right]. \quad (4.27)$$

The apparent horizon in the overdense region is given by

$$\eta = 2\chi \quad \text{and} \quad \eta = 2\pi - 2\chi. \quad (4.28)$$

If we concentrate on type I perturbation, i.e., $0 < \chi_a < \pi/2$, the future apparent horizon corresponds to $\eta = 2\pi - 2\chi$.

The Jeans scale appears in the confrontation between the pressure gradient force and the gravitational force or equivalently between the sound crossing time and the free fall time. The sound wave propagates in the closed Friedmann geometry according to

$$a \frac{d\chi}{dt} = \pm \sqrt{w} c. \quad (4.29)$$

Using Eqs. (4.23) and (4.25), this can be rewritten as

$$\frac{d\chi}{d\eta} = \pm \frac{\sqrt{w}}{1+3w} \quad (4.30)$$

in terms of η and χ . The solutions are given by

$$\eta = \pm \frac{1+3w}{\sqrt{w}} \chi + C_{\pm}, \quad (4.31)$$

where C_{\pm} are constants of integration.

The rarefaction wave starts at the surface $\chi = \chi_a$ of the overdense region at $\eta = 0$ and propagates inwardly to the center. The compression wave also propagates from the center to the surface outwardly, if there is any inhomogeneity within the overdensity. Since the region is initially expanding and the pressure gradient force generally pushes the fluid outwardly, if the sound wave crosses over the overdense region before the maximum expansion, the dynamics of the overdense region may be strongly affected due to the pressure gradient force so that it may not reach the maximum expansion but continue expanding. We can at least expect that the pressure gradient force significantly delays the collapse in this case.

This expectation motivates us to adopt the criterion that if and only if the sound wave crosses from the center to the surface outwardly or from the surface to the center inwardly before the maximum expansion, the pressure gradient force prevents the overdense region from becoming a black hole. This requirement is naturally equivalent to the formation criterion that the sound crossing time over the radius be longer than the free fall time from the maximum expansion to complete collapse. See Fig. 2, which shows the trajectory of the sound wave for the threshold case, where the sound wave crosses over the radius of the overdense region at the same time of the maximum expansion. The present criterion reduces to the following condition:

$$\chi_a > \frac{\pi\sqrt{w}}{1+3w}. \quad (4.32)$$

This means that the Jeans scale R_J at the maximum expansion can be identified with

$$R_J = a_{\max} \sin\left(\frac{\pi\sqrt{w}}{1+3w}\right). \quad (4.33)$$

Therefore, we obtain the following formula for the threshold value of primordial black hole formation:

$$\delta_{Hc}^{\text{UH}} = \sin^2\left(\frac{\pi\sqrt{w}}{1+3w}\right) \quad (4.34)$$

and δ_H^{UH} for primordial black hole formation must satisfy

$$\delta_{Hc}^{\text{UH}} < \delta_H^{\text{UH}} \leq 1. \quad (4.35)$$

This can be considered as a (roughly) necessary and sufficient condition for primordial black hole formation.

Formula (4.34) implies that δ_{Hc}^{UH} increases from 0, reaches a maximum value $\sin^2(\sqrt{3}\pi/6) \simeq 0.6203$ at $w = 1/3$ and decreases to 1/2, as w increases from 0 to 1. δ_{Hc}^{UH} decreases as w increases from 1/3 because of the factor $1/(1+3w)$ on the right-hand side in Eq. (4.30). This factor appears because the dynamical time of the collapse gets shortened by the contribution of the pressure to the source of gravity. δ_{Hc}^{UH} is approximated as $\delta_{Hc}^{\text{UH}} \approx \pi^2 w$ if $w \ll 1$, which is π^2 times the conventionally used Carr's threshold value w , and almost twice for a radiation fluid $w = 1/3$. This means that our analytic formula implies much less production efficiency for $w \ll 1$ and considerably less efficiency for $w = 1/3$ than the conventional estimate. On the other hand, for $w \gtrsim 0.6$, our formula gives a lower threshold value and hence implies higher production efficiency than the conventional estimate.

Although there are many other possible choices for the criterion of black hole formation, the present choice to derive Eq. (4.34) not only is physically natural but also shows a very good agreement with the numerical result as we will see later. To see this more explicitly, we further invent the following two conditions. The one is a stronger formation condition that the future apparent horizon must form before the sound wave crosses over the radius. This leads to

$$\chi_a > \frac{2\pi\sqrt{w}}{1 + 2\sqrt{w} + 3w} \quad \text{or} \quad \delta_{Hc}^{\text{UH}} = \sin^2 \left(\frac{2\pi\sqrt{w}}{1 + 2\sqrt{w} + 3w} \right). \quad (4.36)$$

The other is a weaker condition that the future apparent horizon must form before the sound wave propagates inwardly from the surface to the center and then outwardly back from the center to the surface. This leads to

$$\chi_a > \frac{\pi\sqrt{w}}{1 + \sqrt{w} + 3w} \quad \text{or} \quad \delta_{Hc}^{\text{UH}} = \sin^2 \left(\frac{\pi\sqrt{w}}{1 + \sqrt{w} + 3w} \right). \quad (4.37)$$

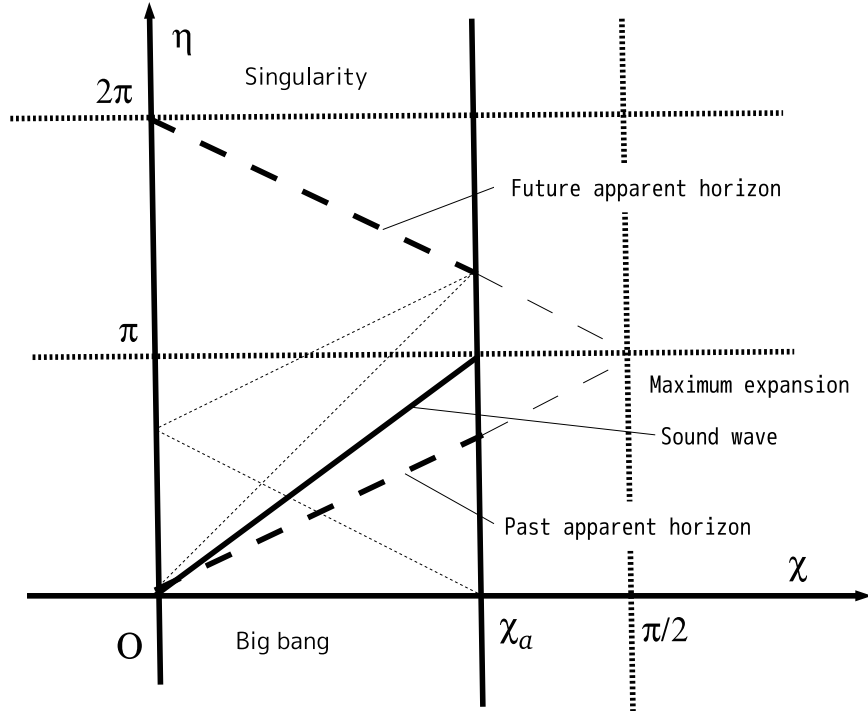


FIG. 2. The trajectories of the sound waves and apparent horizons in the $\eta\chi$ plane for the formation threshold. The sound wave just crosses over the radius of the overdense region from the big bang to the maximum expansion, which is denoted by a thick solid line. The stronger and weaker conditions are also shown by thin dashed lines.

V. COMPARISON WITH THE NUMERICAL RESULT

A. Density perturbation in the comoving slice

We here study the density perturbation in the comoving slice. For this purpose, we need to systematically introduce inhomogeneity, which arises from the big bang universe. Indeed, Polnarev and Musco [13] introduce a time-independent function of r , $K = K(r)$, into the Friedmann–Robertson–Walker metric (3.4) and obtain an asymptotic solution of the Einstein equation in the limit $t \rightarrow 0$, where all the hydrodynamical quantities are nearly homogeneous with their perturbations being small deviations with the small parameter $\epsilon = (R_{H_b}/R_a)^2$ but the curvature perturbations can be arbitrarily large. They call such solutions asymptotic quasihomogeneous solutions. They explicitly obtain the first-order solution in terms of ϵ , which is consistent with a pure growing mode of superhorizon scale in the linear perturbation theory. (See Ref. [29] for higher-order solutions.) They use the first-order solution as initial data to simulate the subsequent nonlinear evolution.

We here give the relationship between the density perturbations in the uniform Hubble slice and in the comoving slice. The combination of Eqs. (32), (41), (57), and (85) of Polnarev and Musco [13] gives the first-order solution for the density perturbation δ in the following form:

$$\delta_1^{\text{COM}} = \frac{3(1+w)}{5+3w} \frac{1}{3r^2} \frac{d}{dr} [r^3 K(r)] r_0^2 \left(\frac{R_{H_b}}{R_a} \right)^2, \quad (5.1)$$

where δ_1^{COM} and r_0 denotes the first-order solution for the density perturbation in the comoving slice and the comoving radius of the overdense region, respectively. For the overdense region in our three-zone model, we have $K(r) = 1$ and $r_0 = \sin \chi_a$, and therefore

$$\frac{1}{3r^2} \frac{d}{dr} [r^3 K(r)] r_0^2 = \sin^2 \chi_a = \delta_H^{\text{UH}}. \quad (5.2)$$

Defining $\tilde{\delta}$ by

$$\tilde{\delta} = \delta_1^{\text{COM}} \left(\frac{R_a}{R_{H_b}} \right)^2, \quad (5.3)$$

we find that this is time-independent and

$$\tilde{\delta} = \frac{3(1+w)}{5+3w} \delta_H^{\text{UH}}. \quad (5.4)$$

$\tilde{\delta}$ is used as the measure of the density perturbation in the numerical simulations in Refs. [12–15]. Note that although $\tilde{\delta}$ is defined in terms of the first-order solution of the asymptotic quasihomogeneous solution, the relation (5.4) between $\tilde{\delta}_c$ and δ_H^{UH} is exact.

B. Comparison with the numerical result

The latest accurate estimate of the threshold value based on fully general relativistic numerical simulations has been given by Musco and Miller [15] for $0.01 \leq w \leq 0.6$. Figure 3 shows the comparison of our analytic formula with the numerical result shown in Fig. 8 of Ref. [15]. Since the numerical result is not so sensitive to the parameter α of the curvature profile function adopted in Ref. [15], we only plot the numerical result for $\alpha = 0$ or a Gaussian profile for clarity. According to Musco and Miller [15], we here present the comparison with the perturbation variable in the comoving slice, $\tilde{\delta}$, which is directly related to the exact density perturbation in the uniform Hubble slice at the moment of horizon crossing, δ_H^{UH} , by Eq. (5.4). In terms of $\tilde{\delta}$, our analytic formula gives

$$\frac{3(1+w)}{5+3w} \sin^2 \left(\frac{\pi\sqrt{w}}{1+3w} \right) = \tilde{\delta}_c < \tilde{\delta} \leq \tilde{\delta}_{\text{max}} = \frac{3(1+w)}{5+3w}. \quad (5.5)$$

In Fig. 3, we plot our analytic formula for the threshold $\tilde{\delta}_c$ together with Carr's original value w and its gauged value $3(1+w)w/(5+3w)$. We also plot our stronger and weaker conditions in the same figure. As we can see in Fig. 3, our analytic formula agrees with the result of the numerical simulations within 20 % approximately for $0.01 \leq w \leq 0.6$. Note that our analytic formula gives $\tilde{\delta}_c \approx 3\pi^2 w/5$ for $w \ll 1$, $(2/3) \sin^2(\sqrt{3}\pi/6) \simeq 0.4135$ for $w = 1/3$ and $3/8$ for $w = 1$. We also find that the numerical result can be qualitatively explained by our sinusoidal function rather than the straight line. For larger values of w ($w \gtrsim 1/3$), our formula appears to systematically underestimate the threshold value. For a radiation fluid ($w = 1/3$), our formula gives a value smaller than the numerical result of Musco and Miller [15] by 10 % approximately. However, we should note that the numerical result also should have dependence on the density profile. It has been reported [13] that the threshold value for a radiation fluid is $\tilde{\delta}_c \simeq 0.45 - 0.47$ and $\simeq 0.48 - 0.66$ depending on the parametrization of curvature profiles as shown in Figs. 10 and 11 of Ref. [13]. This suggests that the 20 % deviation cannot be avoided within our simplified analytic model. Our formula shows a much better agreement for smaller values of w than Carr's original formula and its gauged version, as expected. Even for larger values of w , we can still see that our formula generally shows a better agreement both qualitatively and quantitatively than the gauged version of Carr's formula. We can also see that the numerical result of Musco and Miller [15] is between our stronger and weaker conditions.

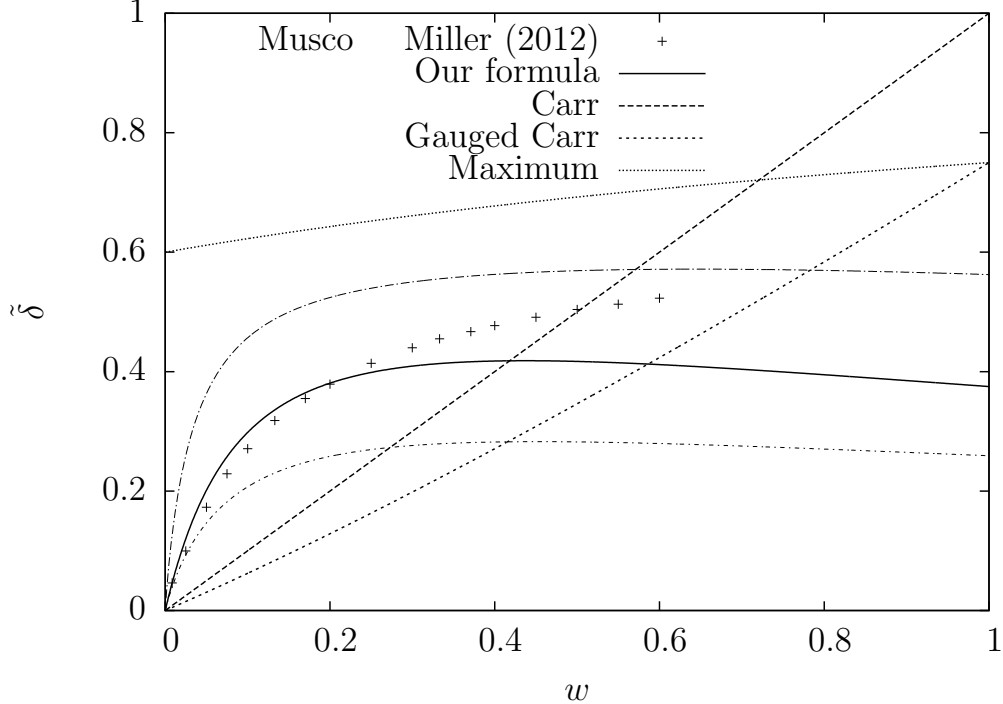


FIG. 3. The threshold values and the maximum value of the density perturbation variable $\tilde{\delta}$ in the comoving slice for different values of w . The crosses plot the result of numerical simulations by Musco and Miller [15] for the profile parameter $\alpha = 0$ or a Gaussian curvature profile. The solid, long-dashed and dashed lines denote the analytic formula obtained in Sec. IV B, Carr’s original formula and its gauged version, respectively. We also plot our stronger and weaker conditions with thin dotted-dashed lines, which are discussed in Sec. IV B. The short-dashed line denotes the geometrical maximum value, corresponding to a three-hemisphere.

Our threshold formula implies that the threshold values are approximately given by $\delta_{Hc}^{\text{UH}} \simeq 0.5 - 0.6$ and $\tilde{\delta}_c \simeq 0.4$ and for $1/3 \lesssim w \lesssim 1$ and are not so sensitive to w in this range. Our formula also suggests that primordial black holes can be formed from type I fluctuations even for very hard equations of state, i.e., $w \simeq 1$, because $\tilde{\delta}_c$ is well below $\tilde{\delta}_{\max}$.

VI. PROBABILITY DISTRIBUTION

Conventionally, it has been assumed that the probability distribution for the density perturbation follows a Gaussian distribution. Then, the fraction $\beta_0(M)$ of the Universe

which goes into primordial black holes of mass scale M at the formation epoch is given by

$$\begin{aligned}
\beta_0(M) &= \int_{\delta_c(M)}^{\delta_{\max}(M)} \frac{2}{\sqrt{2\pi\sigma^2(M)}} \exp\left(-\frac{\delta^2}{2\sigma^2(M)}\right) d\delta \\
&\simeq \operatorname{erfc}\left(\frac{\delta_c(M)}{\sqrt{2}\sigma(M)}\right) \\
&\simeq \frac{\sqrt{2}}{\sqrt{\pi}} \frac{\sigma(M)}{\delta_c(M)} \exp\left(-\frac{\delta_c^2(M)}{2\sigma^2(M)}\right), \tag{6.1}
\end{aligned}$$

where $\sigma(M)$ is the standard deviation of the density perturbation of mass scale M , the factor 2 comes from the Press–Schechter theory, $\operatorname{erfc}(x)$ is the complementary error function and we have assumed $\delta_{\max} \gg \delta_c \gg \sigma(M)$ in the second and last equalities. The last expression is a consequence of the asymptotic expansion of $\operatorname{erfc}(x)$ for $x \gg 1$. In the above expression, M just denotes the mass contained within the overdense region and may be different from the final black hole mass because of possible critical behavior [16] or mass accretion.

However, as we have seen, the density perturbation δ has a finite maximum value and one value of δ generally corresponds to two perturbation configurations, χ_a , the one of type I and the other of type II. The type II fluctuation is nonlinearly large, although δ may be very small. The Gaussian assumption to δ implies the following unreasonable consequence: a linearly small perturbation $\chi_a \simeq 0$, where the overdense region is only slightly bent, and a highly nonlinear perturbation $\chi_a \simeq \pi$, which is nearly separate from the rest of the universe, would be realized with the same probability.

Recently, Kopp, Hofmann, and Weller [6] suggested that the curvature fluctuation is more suitable for the assumption of probability distribution. The curvature fluctuation ζ is defined by the conformal factor of the three metric in the conformally flat form:

$$ds_3^2 = b^2(t)e^{2\zeta(t,s)}(ds^2 + s^2d\Omega^2). \tag{6.2}$$

The averaged curvature fluctuation $\bar{\zeta}$ is defined in Ref. [6] in terms of χ_a as

$$\bar{\zeta} = \frac{1}{3} \ln \frac{3(\chi_a - \sin \chi_a \cos \chi_a)}{2 \sin^3 \chi_a}, \tag{6.3}$$

where $b(t)$ is chosen to be common between the overdense region and the background flat Friedmann region. On the other hand, the peak value of the original variable $\zeta(t, 0)$, which will be denoted just by ζ , can be approximately expressed as [6]

$$\zeta \simeq -2 \ln \cos \frac{\chi_a}{2} \tag{6.4}$$

in the present model, if the contribution from the compensating layer is negligible. $\bar{\zeta}$ and ζ are plotted as functions of χ_a in Fig. 4 of Ref. [6]. ζ (or $\bar{\zeta}$) can be arbitrarily large even for $R_{H_b}/R_a \ll 1$, where the density perturbation δ is sufficiently small. Moreover, unlike δ , ζ monotonically increases from 0 to ∞ as χ_a increases from 0 to π . The threshold value can be derived by substituting $\chi_a = \arcsin \sqrt{\delta_{HC}^{\text{UH}}}$ into the right-hand side of Eq. (6.4). Since any type II fluctuation necessarily has a future apparent horizon immediately after the maximum expansion, the threshold configuration must be of type I and hence $0 < \chi_a < \pi/2$.

We should note that ζ takes a value between 0 and ∞ , that it has one-to-one correspondence with the overdensity configuration χ_a , and that ζ is proportional to δ in the linear regime. For the above three facts, we can naturally extend a Gaussian distribution for ζ (or any other similar curvature variable) to the nonlinear regime, although this needs further justification. As a consequence of this assumption, a linearly small perturbation, i.e., $\chi_a \simeq 0$, is realized with high probability, while a nearly separate universe, i.e., $\chi_a \simeq \pi$, is realized with extremely low probability. That is, we have

$$\begin{aligned} \beta_0(M) &= \int_{\zeta_c(k_{\text{BH}})}^{\infty} \frac{2}{\sqrt{2\pi P_\zeta(k_{\text{BH}})}} \exp\left(-\frac{\zeta^2}{2P_\zeta(k_{\text{BH}})}\right) d\zeta \\ &= \text{erfc}\left(\frac{\zeta_c(k_{\text{BH}})}{\sqrt{2P_\zeta(k_{\text{BH}})}}\right) \\ &\simeq \frac{\sqrt{2P_\zeta(k_{\text{BH}})}}{\sqrt{\pi}\zeta_c(k_{\text{BH}})} \exp\left(-\frac{\zeta_c^2(k_{\text{BH}})}{2P_\zeta(k_{\text{BH}})}\right), \end{aligned} \quad (6.5)$$

where $P_\zeta(k)$ is the power spectrum of ζ , $k_{\text{BH}} = a_b H_b$ at the horizon crossing, and only in the last expression $\zeta_c^2(k_{\text{BH}}) \gg P_\zeta(k_{\text{BH}})$ is assumed. Since $\zeta_c^2 \gg P_\zeta(k_{\text{BH}})$ is usually assumed, it is clear that the precise estimate of the threshold value ζ_c is very important.

For type I fluctuations, we find $0 < \bar{\zeta} < \bar{\zeta}_h = (1/3) \ln(3\pi/4) \simeq 0.2857$, where $\bar{\zeta}_h$ is the value for $\chi_a = \pi/2$. Our analytic formula gives an expression for $\bar{\zeta}_c$ as follows:

$$\bar{\zeta}_c = \frac{1}{3} \ln \frac{3(\chi_a - \sin \chi_a \cos \chi_a)}{2 \sin^3 \chi_a} \Big|_{\chi_a = \pi\sqrt{w}/(1+3w)}. \quad (6.6)$$

For $w \ll 1$, this implies $\bar{\zeta}_c \approx \pi^2 w/10$. Since $\bar{\zeta}_c$ is a monotonically increasing function of χ_a , $\bar{\zeta}_c$ takes a maximum value $\bar{\zeta}_c \simeq 0.08602$ at $w = 1/3$ and $\bar{\zeta}_c = (1/3) \ln[(\pi/2 - 1)/\sqrt{2}] \simeq 0.06377$ at $w = 1$. As for the peak value ζ , we use the approximate expression (6.4). Then, for type I fluctuations, we find $0 < \zeta < \zeta_h = \ln 2 \simeq 0.6931$, where ζ_h is the value for $\chi_a = \pi/2$. Our

analytic formula gives an expression for ζ_c as follows:

$$\zeta_c = -2 \ln \cos \frac{\pi \sqrt{w}}{2(1+3w)}. \quad (6.7)$$

For $w \ll 1$, this implies $\zeta_c \approx \pi^2 w/4$. ζ_c takes a maximum value $\zeta_c \simeq 0.2131$ at $w = 1/3$ and $\zeta_c = -2 \ln \cos(\pi/8) \simeq 0.1583$ at $w = 1$.

Figure 4 plots our analytic formula for the threshold values $\bar{\zeta}_c$ and ζ_c . For $1/3 \lesssim w \lesssim 1$, we find $0.064 \lesssim \bar{\zeta}_c \lesssim 0.086$ and $0.16 \lesssim \zeta_c \lesssim 0.21$, and both are insensitive to w .

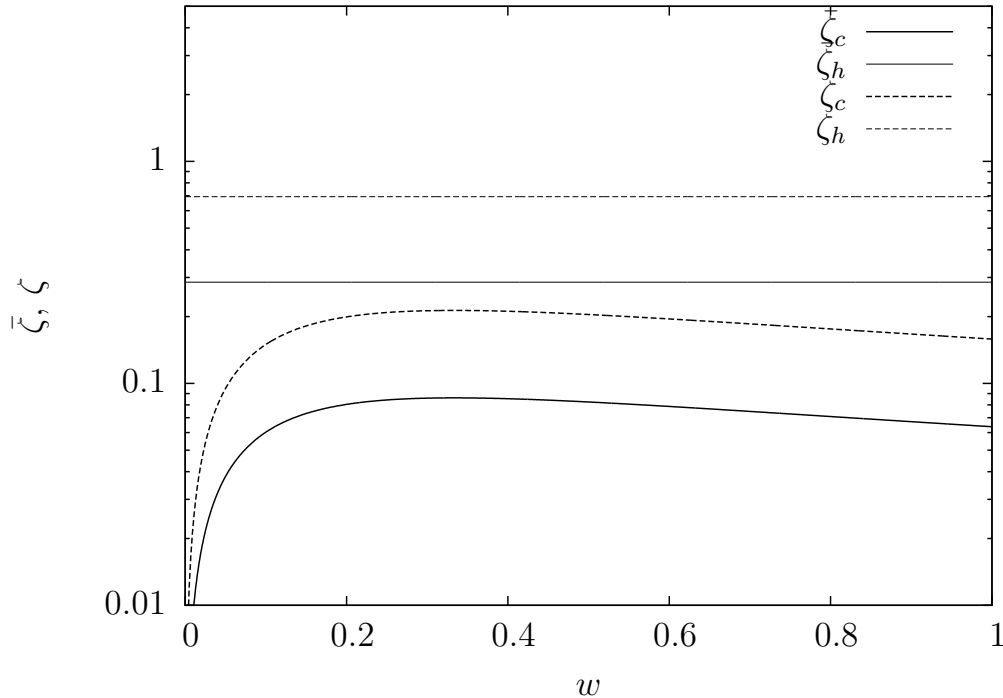


FIG. 4. The threshold values of the curvature perturbations $\bar{\zeta}$ and ζ for different values of w . The lower thick and upper thin solid lines denote our analytic formula for the threshold $\bar{\zeta}_c$ and the value $\bar{\zeta}_h$ for a three-hemisphere, respectively. The lower thick and upper thin dashed lines denote our analytic formula for the threshold ζ_c and the value ζ_h for a three-hemisphere, respectively, under the approximation described in the text. The regions below and above the three-hemisphere line correspond to type I and II fluctuations, respectively, for each of $\bar{\zeta}$ and ζ .

VII. SUMMARY

We have introduced an analytic three-zone model to describe primordial black hole formation. We then applied this model and derived a matter-independent maximum amplitude of density perturbation at the horizon crossing time. Next, we applied the same model to the perfect fluid with the equation of state $p = w\rho c^2$. We then analytically derived a threshold value δ_{Hc}^{UH} for the density perturbation at the horizon crossing in the uniform Hubble slice by a physical argument about the sound waves and the maximum expansion. We clarified the relationship of the density perturbations between the uniform Hubble slice and the comoving slice. Then, we compared the analytic formula to the result of the state-of-the-art numerical simulations from the initial data constructed by the first-order asymptotic quasihomogeneous solutions. We have seen that our analytic formula shows a very good agreement with the result of the numerical simulations and the agreement is generally much better than Carr's formula obtained almost forty years ago. Further analytic and numerical studies on this problem will be extremely important to determine the threshold and the probability of primordial black hole formation and then give the precise prediction for the abundance of primordial black holes for given early Universe scenarios.

ACKNOWLEDGMENTS

The authors would like to thank C. T. Byrnes, B. J. Carr, T. Houri, Tsutomu Kobayashi, H. Maeda, J. C. Miller, I. Musco, T. Nakama, M. Sasaki, and T. Suyama for helpful discussions. The authors were partially supported by the Grant-in-Aid No. 23654082 (T.H.), and Grants No. 21111006, No. 22244030, and No. 23540327 (K.K.) for Scientific Research Fund of the Ministry of Education, Culture, Sports, Science, and Technology, Japan. T.H. was also supported by Rikkyo University Special Fund for Research.

-
- [1] Y. B. Zel'dovich and I. D. Novikov, *Sov. Astron.* **10**, 602 (1967).
 - [2] S. Hawking, *Mon. Not. R. Astron. Soc.* **152**, 75 (1971).
 - [3] B. J. Carr, *Astrophys. J.* **201**, 1 (1975).
 - [4] B. J. Carr, K. Kohri, Y. Sendouda, and J. 'i. Yokoyama, *Phys. Rev. D* **81**, 104019 (2010).

- [5] B. J. Carr and S. W. Hawking, *Mon. Not. R. Astron. Soc.* **168**, 399 (1974).
- [6] M. Kopp, S. Hofmann, and J. Weller, *Phys. Rev. D* **83**, 124025 (2011).
- [7] B. J. Carr and T. Harada (unpublished).
- [8] D. K. Nadezhin, I. D. Novikov, and A. G. Polnarev, *Sov. Astron.* **22**, 129 (1978).
- [9] I. D. Novikov and A. G. Polnarev, *Sov. Astron.* **24**, 147 (1980).
- [10] J. C. Niemeyer and K. Jedamzik, *Phys. Rev. D* **59**, (1999) 124013.
- [11] M. Shibata and M. Sasaki, *Phys. Rev. D* **60**, 084002 (1999).
- [12] I. Musco, J. C. Miller, and L. Rezzolla, *Classical Quantum Gravity* **22**, 1405 (2005).
- [13] A. G. Polnarev and I. Musco, *Classical Quantum Gravity* **24**, 1405 (2007).
- [14] I. Musco, J. C. Miller, and A. G. Polnarev, *Classical Quantum Gravity* **26**, 235001 (2009).
- [15] I. Musco and J. C. Miller, arXiv:1201.2379v3.
- [16] J. C. Niemeyer and K. Jedamzik, *Phys. Rev. Lett.* **80**, 5481 (1998).
- [17] M. Y. Khlopov and A. G. Polnarev, *Phys. Lett. B* **97**, 383 (1980).
- [18] T. Suyama, T. Tanaka, B. Bassett, and H. Kudoh, *Phys. Rev. D* **71**, 063507 (2005) 063507.
- [19] T. Suyama, T. Tanaka, B. Bassett, and H. Kudoh, *J. Cosmol. Astropart. Phys.* 04 (2006) 001.
- [20] L. Alabidi, K. Kohri, M. Sasaki, and Y. Sendouda, *J. Cosmol. Astropart. Phys.* 09 (2012) 017.
- [21] L. Alabidi, K. Kohri, M. Sasaki, and Y. Sendouda, *J. Cosmol. Astropart. Phys.* 05 (2013) 033.
- [22] V. A. Belinsky, I. M. Khalatnikov, and E. M. Lifshitz, *Adv. Phys.* **31**, 639 (1982).
- [23] V. A. Belinsky, I. M. Khalatnikov, and E. M. Lifshitz, *Adv. Phys.* **19**, 525 (1970).
- [24] T. Harada and B. J. Carr, *Phys. Rev. D* **71**, 104009 (2005).
- [25] R. M. Wald, *General Relativity* (Chicago University Press, Chicago, IL, 1984).
- [26] C. W. Misner and D. H. Sharp, *Phys. Rev.* **136**, B571 (1964).
- [27] S. A. Hayward, *Phys. Rev. D* **53**, 1938 (1996).
- [28] S. W. Hawking and G. F. R. Ellis, *The Large scale structure of space-time* (Cambridge University Press, Cambridge, England, 1973).
- [29] A. G. Polnarev, T. Nakama, and J. i. Yokoyama, *J. Cosmol. Astropart. Phys.* 09 (2012) 027.